Static Space-charge Distributions

J. ROSS MACDONALD

Texas Instruments Incorporated, Dallas 9, Tex.

Introduction

Whenever the motion of electric charge in a solid or liquid under the influence of an electric field is partly or completely impeded at an electrode, a space-charge region forms near the electrode. Such charges may occur because of thermal or photoexcitation of the intrinsic material or of impurities in it, because of high-field emission or breakdown at one electrode, during the molding of insulating high polymers, etc. Measurement of the spatial dependence of potential within the material and of the space-charge capacitance as functions of applied external potential can yield valuable information concerning the nature and concentrations of charge carriers within the material, and of recombination and breakdown properties.

Although the nonlinear transient processes occurring after the application or removal of potential from a charge-containing material with one or two blocking electrodes have not been satisfactorily treated,[1] some exact solutions for static space-charge distributions have been given.[2, 3, 4, 5] The exact solutions apply to the cases where charges of both signs are mobile for a finite-length, one-dimensional sample between two blocking electrodes [2, 3] and for a semi-infinite sample with blocking electrode at the origin.[4] In the present work these solutions will be compared with the case where mobile charge of only one sign is present but where recombination may occur with fixed charges of opposite sign.

There are many experimental situations in solids where it is more likely that charge of only a single sign is mobile than that charges of both signs move. Even in the latter case when the two mobilities are widely different, a quasistatic distribution will be initially set up which will be like that occurring when charge of only one sign is mobile.[3] Examples of materials for which the present treatment is likely to apply when one or more blocking electrodes are used are : electroluminescent materials, photoconducting alkali and silver halides,[6, 7, 8, 9] impure ice,[10] plastic insulators,[11] electrets,[12] and glass.[13, 14] Finally, the treatment should apply, at least approximately, to extrinsic semiconductors. It should be emphasized that the univalent charges considered need not be electrons or holes but can be protons, other ions, charged impurities, etc.

The mobile charge with which we shall be concerned is assumed to arise from ionization of neutral impurity centers in the material and from injection at any non-blocking electrode. When injection or extraction occurs, the material as a whole will not be neutral. We shall assume for simplicity that there are no neutral traps in the material which can capture mobile charge and become charged but that all recombination is bimolecular, between mobile charge and ionized impurity centers.

Solution of the Space-Charge Equations

Let us consider unit cross-section of charge-containing material extending from a plane, blocking electrode at $x = 0$ to $x = l$. It will be assumed that the electrode at $x = l$ is essentially ohmic if $l = \infty$ so that mobile charge can enter or leave the material there without space-charge formation. If l is finite, both electrodes are taken blocking. For simplicity, we shall specify that any blocking-electrode contact or surface potential shall be included in the applied potential ψ_0; thus, when ψ is zero throughout the material, it will be electrically neutral throughout. Discussions of inner and electrochemical potential pertinent to the present case have been given by Skinner [5] and Grahame.[15]

The pertinent differential equations for charge motion under the influence of an electric field in a solid or liquid may be written for a one-dimensional system with bimolecular recombination as [2, 16]

$$\frac{\partial n}{\partial t} = k_1 n_c - k_2 np + D_n \frac{\partial^2 n}{\partial x^2} + \mu_n \frac{\partial (nE)}{\partial x} \tag{1}$$

$$\frac{\partial p}{\partial t} = k_1 n_c - k_2 np + D_p \frac{\partial^2 p}{\partial x^2} - \mu_p \frac{\partial (pE)}{\partial x} \tag{2}$$

$$\frac{\partial n_c}{\partial t} = - k_1 n_c + k_2 np \tag{3}$$

$$\frac{\partial E}{\partial x} = \frac{4\pi e}{\epsilon} (p - n) \tag{4}$$

$$E = - \frac{d\psi}{dx} \tag{5}$$

In these equations, n_c is the concentration of neutral impurity centers, k_1 and k_2 are dissociation and recombination rate constants, and the other symbols have their conventional meanings. The condition that both positive and negative charge be blocked at an electrode is that of zero positive and negative currents,

$$\left.\begin{aligned} \mu_p pE - D_p \frac{\partial p}{\partial x} &= 0 \\ \mu_n nE + D_n \frac{\partial n}{\partial x} &= 0 \end{aligned}\right\} \text{at electrode} \tag{6}$$

Let us now specialize the foregoing equations for the static case and for negative charges only mobile. Note that in the static case, the dielectric constant ϵ in (4) is the low-frequency limiting value of the differential dielectric constant of the material in the absence of free charges.[17] As long as the dielectric constant is independent of field strength, the static and differential dielectric constants are equal; this will be assumed to be the case in the present treatment. After an integration of (1), which can be readily carried out because the currents in the blocking static case are zero,[4] we obtain, on using the Einstein relation,

$$\frac{dn}{dx} = - \left(\frac{e}{kT}\right) En \tag{7}$$

Equation (3) becomes [16]

$$k_2 np = k_1 (N - p) \tag{8}$$

where N is the homogeneous concentration of neutral centers before any dissociation is assumed to have occurred. The concentration of neutral centers in a region where the concentration of fixed positive centers is $p(x)$ must be simply $(N - p)$ as in (8), since the positive charge concentration p is assumed to arise entirely by dissociation from neutral centers.

Before solution of the above equations, it will be helpful to normalize the quantities of interest. Define the Debye length for a concentration N of charges of one sign mobile as $L_{D1} = [\epsilon kT/4\pi e^2 N]^{\frac{1}{2}}$. This is the minimum Debye length and arises when all neutral centers are ionized. When there is incomplete ionization and non-zero recombination, the effective Debye length (abbreviated EDL), L_e, will be greater, since the concentration of mobile charge is then decreased. In such a case let $L_e \equiv \theta L_{D1}$, where the correction factor θ, not a function of position, will be determined later. Let $\hat{\psi} \equiv \psi/(kT/e)$; $\hat{n} \equiv n/N$; $\hat{p} \equiv p/N$; $\hat{E} \equiv E/(kT/eL_e)$; $R \equiv k_2 N/k_1$; $z \equiv x/L_{D1}$; $L = l/L_{D1}$; $\hat{x} = x/L_e$; $\hat{L} = l/L_e$.

The quantity z is a measure of distance in terms of the number of fixed minimum Debye lengths, while $\hat{x}$ measures the number of effective Debye lengths, the quantity of greater interest. Note that the recombination ratio R depends only on material properties. When R is zero, there is no recombination.

Written in terms of normalized variables, the pertinent equations become

$$\frac{d\hat{n}}{d\hat{x}} = -\hat{E}\hat{n} \tag{7'}$$

$$\frac{d\hat{E}}{d\hat{x}} = \theta^2(\hat{p} - \hat{n}) \tag{4'}$$

$$\hat{E} = -\frac{d\hat{\psi}}{d\hat{x}} \tag{5'}$$

$$\hat{p} = [1 + R\hat{n}]^{-1} \tag{8'}$$

Eq. (6) is automatically satisfied since there is no current anywhere in the system.

The above set of equations can be partly solved by substituting (8') in (4'), differentiating (7') with respect to $\hat{x}$, and eliminating $\hat{E}$ and $d\hat{E}/d\hat{x}$ from the resulting equation using (4') and (7'). The resulting second-order nonlinear differential equation in $\hat{n}$ can be transformed to a linear Bernoulli equation, then integrated directly. The result is

$$\left(\frac{1}{\hat{n}}\frac{d\hat{n}}{d\hat{x}}\right)^2 = A + 2\theta^2 \ln\left\{\frac{1 + R\hat{n}}{\hat{n}}\right\} \tag{9}$$

On using (7'), this equation may be written

$$(\hat{E})^2 = A + 2\theta^2\left\{\hat{n} + \ln\left(\frac{1 + R\hat{n}}{\hat{n}}\right)\right\} \tag{9'}$$

where A is an integration constant.

By combining Eqs. (7') and (5'), one can obtain

$$\frac{1}{\hat{n}}\frac{d\hat{n}}{d\hat{x}} = -\hat{E} = \frac{d\hat{\psi}}{d\hat{x}} \tag{10}$$

Let $\hat{n} = \hat{n}_\infty$ at some potential $\hat{\psi}_d$ which occurs a distance $\hat{x}_d$ from the

electrode at $\hat{x} = 0$, where $\hat{\psi} = \hat{\psi}_0$. Then (10) yields

$$\hat{n} = \hat{n}_\infty e^{\hat{\psi}-\hat{\psi}_d} \equiv \hat{n}_\infty e^{\hat{\phi}} \tag{11}$$

where $\hat{\phi}$ is a new potential variable. $\hat{n}_\infty$ is the common equilibrium value of $\hat{n}$ and $\hat{p}$ in the absence of space-charge. From (8′) it is

$$\hat{n}_\infty = -\frac{1}{2R} + \left[\left(\frac{1}{2R}\right)^2 + \frac{1}{R}\right]^{\frac{1}{2}} \tag{12}$$

a reasonably well-known equation. We shall show later that

$$\theta = [\hat{n}_\infty(2 - \hat{n}_\infty)]^{-\frac{1}{2}}.$$

In the semi-infinite case $\hat{n} = \hat{n}_\infty$ only at $\hat{x} = \infty$ where $\hat{\psi} = 0$. Thus, $\hat{\psi}_d = 0$ also and $\hat{\phi} \equiv \hat{\psi}$. On the other hand, in the finite length case it turns out that $\hat{x}_d \leqslant \hat{L}/2$ and $\hat{\psi}_0 < \hat{\psi}_d \leqslant \hat{\psi}_0/2$. Since we shall always take $\hat{\psi} = 0$ at $\hat{x} = \hat{L}$, the values of $\hat{\phi}$ at the two electrodes will be $\hat{\phi}_0 = \hat{\psi}_0 - \hat{\psi}_d$ and $\hat{\phi}_l = -\hat{\psi}_d$. Only in the case of carriers of both sign effectively mobile is $\hat{\psi}_d = \hat{\psi}_0/2$ and $\hat{x}_d = \hat{L}/2$. Then the potential distribution will be antisymmetrical about the $\hat{x} = \hat{x}_d$ line.

Introducing (11) and the relation $\hat{n}_\infty = (1 + R\hat{n}_\infty)^{-1}$, the electric field can be written as a function of $\hat{\phi}$ as

$$\hat{E}(\hat{\phi}) = \pm\sqrt{2}\theta[c_0 + \hat{n}_\infty(e^{\hat{\phi}} - 1) + \ln\{1 + \hat{n}_\infty(e^{-\hat{\phi}} - 1)\}]^{\frac{1}{2}} \tag{13}$$

where c_0 is a new integration constant related to A by

$$A = 2\theta^2(c_0 - \hat{n}_\infty + \ln \hat{n}_\infty^2)$$

and the sign is selected such that the field is directed from positive to negative charges. The reason for casting the integration constant in this form is that it allows us to subsume both the infinite and finite length cases together in a single formula. In the former, $\hat{E}$ is zero at $\hat{x} = \infty$ where $\hat{\psi} = 0$. Eq. (13) therefore requires that c_0 be zero in this case. Alternatively, when $c_0 > 0$, l will be less than infinite.

Next, $\hat{\psi}_d$ must be determined for the finite-length case. On integrating (4) from 0 to L, the condition of overall space-charge neutrality ensured by the blocking character of both electrodes leads to

$$\int_0^{\hat{L}} \frac{d\hat{E}}{d\hat{x}}\, d\hat{x} = 0 \tag{14}$$

so that

$$\hat{E}(\hat{\phi}_0) \equiv \hat{E}(\hat{\psi}_0 - \hat{\psi}_d) = \hat{E}(\hat{\phi}_l) \equiv \hat{E}\,(-\hat{\psi}_d) \tag{15}$$

This necessary equality between the fields at the two electrodes is the main reason for the essential differences between the finite and infinite length cases. No matter how great l is, the electrode fields are equal in the finite case, but because of the ohmic electrode assumed in the infinite length case, the field at this electrode is always zero.

When Eqs. (15) and (13) are combined, the following transcendental equation for $\hat{\psi}_d$ is obtained

$$\hat{\psi}_d = \hat{\psi}_0 - \ln\left\{\frac{\ln\left[\dfrac{1 + \dfrac{e^{\hat{\psi}_d}}{R\hat{n}_\infty}}{1 + \dfrac{e^{-(\hat{\psi}_0-\hat{\psi}_d)}}{R\hat{n}_\infty}}\right]}{\hat{n}_\infty(1 - e^{-\hat{\psi}_0})}\right\} \tag{16}$$

In the $R = 0$ case, (16) becomes

$$\hat{\psi}_d = \hat{\psi}_0 - \ln [\hat{\psi}_0/(1 - e^{-\hat{\psi}_0})] \tag{17}$$

For $R > 0$, $\hat{\psi}_d$ is less than the value given in (17) for the same applied potential. In the two limiting cases $e^{\hat{\psi}_d} >> R\hat{n}_\infty$ and $e^{\hat{\psi}_d} << R\hat{n}_\infty$, (16) can be considerably simplified but it still remains transcendental. Finally, it can be shown from (16) that as $R \to \infty$ or $\hat{\psi}_0 \to 0$, $\hat{\psi}_d \to \hat{\psi}_0/2$. Note that $\hat{\psi}_d$ is a function of $\hat{\psi}_0$ and R but not of $\hat{L}$.

Eq. (5′) can be written as

$$\hat{x} = \frac{x}{L_e} = \int_{\hat{\phi}}^{\hat{\phi}_0} \frac{d\hat{\phi}}{|\hat{E}(\hat{\phi})|} \tag{18}$$

where $\hat{E}(\hat{\phi})$ is given by (13). This is the formal solution of the problem and is complete in the infinite case. For $l < \infty$, however, c_0 remains to be determined. If we let $\hat{\phi} = \hat{\phi}_l$ in (18) we obtain

$$\hat{L} = \frac{l}{L_e} = \int_{\hat{\phi}_l}^{\hat{\phi}_0} \frac{d\hat{\phi}}{|\hat{E}(\hat{\phi})|} \tag{19}$$

an implicit, transcendental equation for c_0. For the present case of immobile charge of one sign, (18) and (19) cannot be integrated in closed form.

When charges of both signs are mobile and there is no recombination, the static space-charge distribution equations can be solved exactly. For the one-blocking-electrode semi-infinite case, the result is [4]

$$\hat{\psi} = 4 \tanh^{-1}\{e^{-\hat{x}} \tanh (\hat{\psi}_0/4)\} \tag{20}$$

where L_e is here $(L_{D1}/\sqrt{2}) \equiv L_{D2}$. In the two-blocking-electrode, finite-length case, the result must be expressed in terms of Jacobian elliptic functions [1, 2, 18] which are poorly tabulated in the regions of most present interest.

In the present case, an IBM 650 digital computer has been used to make all the pertinent calculations to a high degree of accuracy. Eqs. (16) and (19) have been solved by iteration and the results used in (18) to yield the dependence of potential on distance in various cases of interest. In the semi-infinite case, only (18) by itself need be used. When a computer is not available, various approximate solutions may be obtained which are useful over at least part of the range of $\hat{x}$. In particular, it is found that when $\hat{n}_\infty(e^{-\hat{\phi}} - 1) \ll 1$, (18) simplifies to yield the two two-mobile solutions already mentioned. These solutions involve $\hat{n}_\infty$ rather than N in L_{D2}, however. For $\hat{n}_\infty \ll 1$, it is necessary that R be large ; such large recombination can effectively mobilize the fixed charges, making charges of both signs essentially mobile.

Two other cases are of interest. When $e^{\hat{\phi}} \gg 1$ or c_0 whichever is the larger, the integration in (18) can be carried out to yield

$$\hat{x} \cong \frac{2}{\theta\sqrt{2\hat{n}_\infty}}[e^{-\hat{\phi}/2} - e^{-\hat{\phi}_0/2}] \tag{21}$$

In this case, mobile charge builds up at the $\hat{x} = 0$ electrode and a charge accumulation region forms near the electrode. For large R, $(\hat{n}_\infty\theta^2/2)^{\frac{1}{2}}$ approaches 1/2. When $\hat{\phi}$ is large and negative and $|\hat{\phi}| \gg |c_0 - \hat{n}_\infty + \ln \hat{n}_\infty|$

or 1 whichever is the larger, (18) leads to

$$\hat{x} \cong \frac{\sqrt{2}}{\theta}\{[\hat{\phi}_0 - \hat{n}_\infty + \ln \hat{n}_\infty + c_0]^{\frac{1}{2}} - [\,|\,\hat{\phi}\,| - \hat{n}_\infty + \ln \hat{n}_\infty + c_0]^{\frac{1}{2}}\} \qquad (22)$$

This result is useful in delineating most of the exhaustion and depletion region that forms in the neighborhood of a blocking electrode when the potential causes mobile charge to be withdrawn from this region.

In the finite length case, the potential distribution between electrodes must finally become linear for very high recombination ratios (little mobile charge) or for lengths less than L_{D1}. In such a case c_0 is the dominant quantity in $\hat{E}(\hat{\phi})$ and approaches its largest value, which, from (19), must be

$$c_{0\max} = \tfrac{1}{2}\left(\frac{\hat{\psi}_0}{\theta \hat{L}}\right)^2 = \tfrac{1}{2}\left(\frac{\hat{\psi}_0}{L}\right)^2 \qquad (23)$$

The smallest value of c_0 is zero. For fixed R and appreciable $\hat{L}$, it is found that $c_0 \propto e^{-\hat{L}}$. Also, for fixed $\hat{L}$ and appreciable R it turns out that $c_0 \propto \theta^{-2} \simeq R^{-\frac{1}{2}}$ as in (23).

Discussion of Static Distribution Curves

(1) single blocking electrode

Figs. 1 through 4 illustrate space charge behavior for various conditions. The curves of these figures have been calculated from Eq. (18) using an

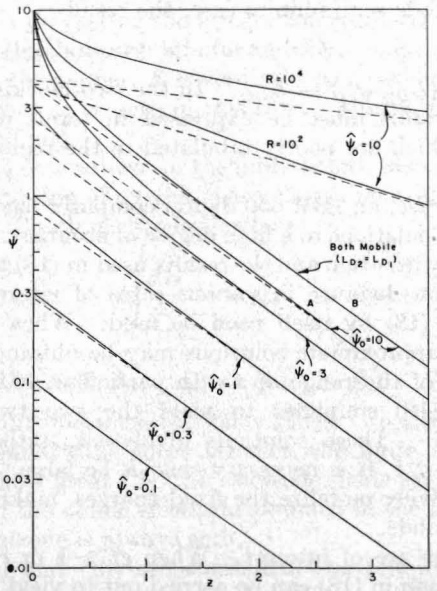

Fig. 1. Accumulation region potential curves for various values of applied potential versus normalized distance. The six lower curves are for $R = 0$.

IBM 650 computer.[19] Although we only show the dependence of $\hat{\psi}$ on normalized distance, that of $\hat{n}$, $\hat{p}$, and $\hat{E}$ can be obtained using the $\hat{\psi}$ results and Eqs. (11), (12), (8′), and (13). Fig. 1 illustrates the development of a charge accumulation region as the applied potential is increased from very

small values. In this figure, all but the top two curves are for $R = 0$. Note that the curve for $\hat{\psi} = 0{\cdot}1$ is a good exponential, but that the other curves progressively deviate from exponential behavior in the small z region as $\hat{\psi}_0$ increases.

The two top curves show how the space-charge region is spread out for non-zero recombination. Since the abscissa is here z, the normalization of distance is constant independent of R. Were the top two curves replotted versus $\hat{x}$ so that comparison could be made on the basis of an equal number of effective Debye lengths (depending on R through θ), both top curves would fall between the curves marked A and B in the figure. For $R = 10^8$, the resulting curve is indistinguishable from B, that for the case where both positive and negative charges are mobile. Since curves for all R values fall in the narrow region between A and B, we see that on comparing in terms of effective Debye lengths, R has only a small effect on the space-charge distribution in the accumulation case.

When $\hat{\psi}_0$ is greater than about 10 (equivalent to approximately 0·25 volts at room temperature), the accumulation region builds up only in the region of very small z ($< 0{\cdot}1$) and the rest of the curve remains the same as that for $\hat{\psi} = 10$. We have not illustrated accumulation region curves for large values of $\hat{\psi}_0$ for two reasons. First, for small R, they lead to exceptionally high fields and charge concentrations at $\hat{x} = 0$.[3] Experimentally, high-field emission, dielectric saturation, etc., will occur before such fields and concentrations are reached. For $R = 0$, $\hat{\psi}_0 = 20$ leads to a normalized field $\hat{E}_0 = 3{\cdot}12 \times 10^4$ at $\hat{x} = 0$. At room temperature, this corresponds to an actual field of $8{\cdot}10^6$ volts/cm. for an effective Debye length of 10^{-4} cm. It may also be pointed out that high fields may have an effect on recombination and emission [20] and that the concept of electron motion in a conduction band is itself not useful if the field is very high.[21] Finally, it should be mentioned that for high $\hat{\psi}_0$ the mathematics may call for not only exceptionally high charge concentrations at the electrode but extremely rapid decrease in the concentration as z increases from zero. It is clear that the physical situation will not conform to the mathematical solution if the mean free path of the mobile charges is greater than the distance in which $\hat{\psi}$ and $\hat{n}$ are required to change appreciably. In this case, the terms which describe diffusion in the equations will certainly be inapplicable.

When R is very great, the situation is somewhat different. The large value of R produces a small value of $\hat{n}_\infty$, and the field and charge concentration at the blocking electrode will not necessarily be excessive. In terms of $\hat{x}$, the decay of $\hat{\psi}$ away from the electrode will still be very rapid but L_e may be so large that the decay will actually take place over appreciable distances. As an example, consider the case $R = 10^{40}$, $\hat{\psi}_0 = 50$. Then $\hat{n}_\infty = 10^{-20}$. If $N = 10^{18}$ cm^{-3}, for example, the material is essentially insulating. The quantity θ is $10^{10}/\sqrt{2}$ and even for an L_{D_1} of 10^{-7} cm., L_e is $7{\cdot}10^2$ cm. For this same L_{D_1}, the field at the electrode is $2{\cdot}6 \times 10^6$ volts/cm. The normalized potential drops from 50 to 20 in $6{\cdot}4 \times 10^{-2}$ cm. and to 10 in 32 cm. At the latter point, $\hat{n}$ is $2{\cdot}2 \times 10^{-16}$. Because of the very few free carriers present in material with such a high recombination ratio, it may be difficult to measure the dependence of potential on distance from the blocking electrode even though the distance scale is favorable.

Fig. 2 illustrates the progressive formation of a depletion and exhaustion

region at the blocking electrode when fields are present which draw the mobile charge away from the electrode. The dotted line on the $\hat{\psi}_0 = -10$ curve is calculated from Eq. (22) ; for $|\hat{\psi}| > 2$, this equation fits the curves of the figure extremely well. The mathematical solution calls for extremely small but non-zero $\hat{n}$ values when $\hat{\psi} \ll -1$. For example, at $\psi = -100$

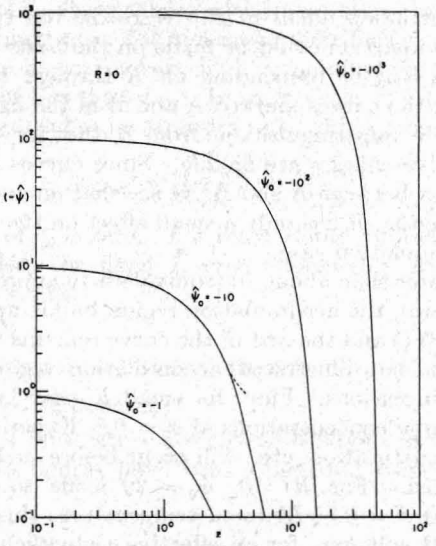

FIG. 2. Exhaustion-depletion region potential-distance curves for various values of applied potential. The dotted line represents an approximate expression.

and $R = 0$, $\hat{n} \simeq 4 \cdot 10^{-44}$. This value is completely negligible and can be replaced by zero with no effect on the potential distribution. Because $\hat{n}$ is so small in the exhaustion region, recombination has little effect on the curves in this region using the z scale. Thus, for $\hat{\psi}_0 = -1000$, $z = 37.10$ at $\psi = -30$ for $R = 0$ and is 39.52 at $\hat{\psi} = -30$ for $R = 10^{16}$.

The present treatment is based on the assumption of a continuous space charge. For it to apply, it is necessary that the exhaustion region thickness be large compared to the average distance between ionized centers, $N^{-1/3}$ cm. From (22) the approximate exhaustion layer thickness ($|\hat{\psi}_0| \gg |\ln \hat{n}_\infty - \hat{n}_\infty|$) is $L_{D_1}\sqrt{2|\hat{\psi}_0|} = [\epsilon |\psi_0| / 2\pi e N]^{\frac{1}{2}}$. Thus, the exhaustion layer solution is only a good approximation when this quantity is at least five or ten times greater than $N^{-1/3}$. Taking the factor as 10, we obtain the condition for validity, $|\psi_0| \geqslant 200\, \pi e N^{1/3}/\epsilon$.

The strong exhaustion regions illustrated in Fig. 2 are very similar to those found with reversed-biased p-n junctions. Mathematically, the mobile charge concentration in the exhaustion region follows the Maxwell-Boltzmann distribution of Eq. (11) and reaches extremely small values. Physically, it will actually be zero over most of the region. In the region of very low concentration, the diffusion terms in the equations will not be applicable and the field will withdraw all mobile charge from most of the exhaustion region.

Fig. 3 illustrates the initial setting up a depletion region starting from very small $\hat{\psi}_0$. These curves should be compared with the corresponding

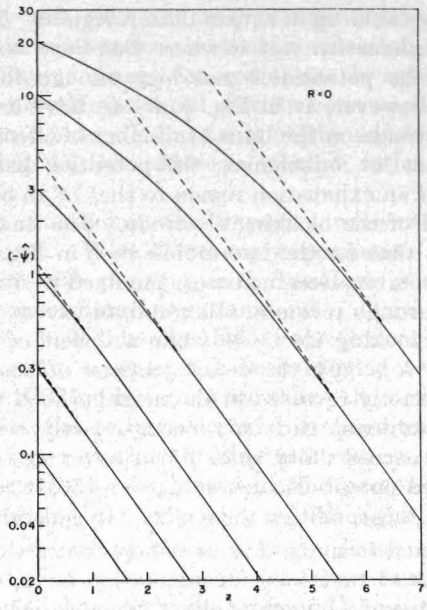

FIG. 3. Potential-distance curves showing the initial formation of a depletion-exhaustion region for low applied potentials.

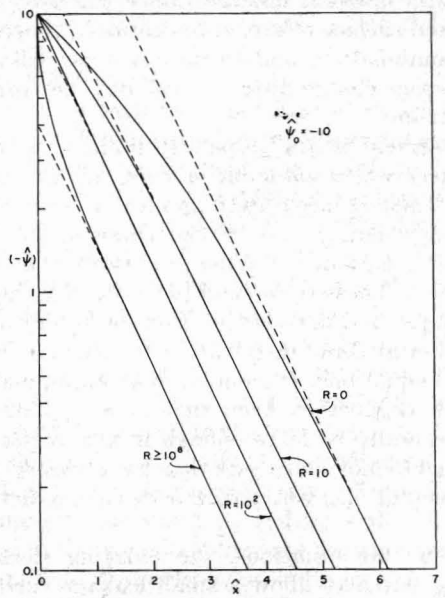

FIG. 4. Exhaustion region potential-distance curves for $\hat{\psi}_0 = -10$ and various values of R. Distance scale measures number of effective Debye lengths and normalization is therefore a function of R.

ones of Fig. 1 for the build up of accumulation regions. The effect of $R > 0$ is negligible in an exhaustion region where there are no mobile charges to recombine. When the potential is not high enough to produce complete charge exhaustion, however, as in Fig. 4, R can have an appreciable effect when comparison is made on the basis of number of effective Debye lengths. It will be noted that as R increases, the potential distribution gradually changes from that of an exhaustion region to that of an accumulation region in the neighborhood of the blocking electrode. The final $R \geqslant 10^8$ curve is exactly the same as that for the two-mobile case in Fig. 1 and is described by Eq. (20). As recombination increases, the fixed positive charges become essentially mobile through recombination and an excess of them (but $\leqslant N$) build up near the blocking electrode while a deficit of negative charge is formed there. For $R \geqslant 10^8$, the concentrations of positive and negative charge are almost exactly reversed in the neighborhood of the electrode for $\hat{\psi}_0 = \pm 10$. Such reversal can only occur exactly when the maximum value of $\hat{n}$ does not exceed unity since $\hat{p}$ can never exceed this value. For very negative applied potentials such as $\hat{\psi}_0 = -50$, it requires values of R such as 10^{50} to cause this condition to be met. In general, for $\hat{n}_{\max} = \hat{n}_\infty \cdot e^{\hat{\phi}_0}$ to be less than or equal to unity it is necessary that $e^{\hat{\phi}_0} \leqslant \sqrt{R}$, for large R. For a depletion layer to turn to an accumulation layer, the same condition with the absolute value of $\hat{\psi}_0$ taken applies. Since $\hat{\psi}_0 = -1000$ corresponds to only about -25 volts at room temperature, the maximum value of R found experimentally will usually not be great enough for the above condition to hold for most applied potentials.

Various conditions under which the mathematical solution does not correspond to a physically realizable situation have already been noted. It should additionally be pointed out that since the present solution is one-dimensional, edge and surface effects are neglected. There will be situations where surface recombination and surface states will exert appreciable influence on static space-charge distributions, but they are outside the scope of the present treatment.

The present treatment is also implicitly limited to Maxwell-Boltzmann statistics. In samples where electrons or holes are the mobile carriers, the present solution will not be accurately applicable when mobile charge concentrations reach degeneracy, and Fermi-Dirac statistics must be used. Two cases may be mentioned. When n_∞ is in the degenerate region, the Einstein relation between μ and D will not hold but must be replaced, e.g. in Eq. (7), and in the expression for L_{D1} by a relation involving integrals over the Fermi-Dirac distribution function. This greatly complicates solution of the equations. Secondly, in an accumulation region, n may be large enough for degeneracy even though n_∞ is not. In this case, the electric field will generally be large enough in this region (provided breakdown or saturation has not occurred) that band-theory will not be applicable [21] and the values of $n(x)$ will depart from the predictions of the present solution.

In some experimental situations, the blocking electrode may not be completely blocking but may allow a small leakage current to flow on the application of a potential difference to the material. Additionally, in semiconductors intrinsic generation of mobile holes and electrons will contribute charges not considered in the present theory. These sources of additional

charge will usually not alter the charge distribution appreciably in the regions where the normal space-charge concentration is high. They may determine the minimum charge concentrations in exhaustion regions, but are not likely to alter the potential distributions appreciably. As long as the additional charge is small, the fields of the present treatment may be considered as acting on the additional charge without themselves being much changed by it.

In the present treatment, the impurity concentration N has been assumed homogeneous. Were there any experimental reason to expect it to vary appreciably with position, such variation could be readily incorporated into the space-charge equations and a digital computer solution produced with little more difficulty than in the present case.

Finally, the present solution has been applied to a sample of semi-infinite length. As the foregoing curves show, the actual length necessary for the internal potential to have decayed in magnitude by a factor of 10 or more from its value at the blocking electrode is no more than three effective Debye lengths for an accumulation region and approximately (from Eq. (22)) $\sqrt{2 \mid \hat{\psi}_0 \mid}\ L_{D_1}$ lengths for an exhaustion region. If an ohmic contact is placed along the specimen a distance equal or greater to those above instead of at $\hat{x} = \infty$, the actual space-charge distribution in the portion of the sample between the blocking and ohmic contacts will be little altered. The potential distribution need not be altered at all for even shorter lengths provided the added electrode is not exactly ohmic. All that is necessary is to add an electrode at whatever the desired distance that will ensure duplication of the infinite-length-solution field, potential, and charge concentrations at the point of addition. Such an electrode will not be ohmic, since it will have a potential drop across it equal to the potential difference from the point of addition to $\hat{x} = \infty$ in the infinite-length solution.

(2) TWO BLOCKING ELECTRODES

The finite-length case with two blocking electrodes is both similar and dissimilar to the semi-infinite, one-blocking-electrode case. It is similar in that charge will be drawn away from one electrode forming a depletion or exhaustion region there and will build up at the other electrode producing an accumulation region in its neighborhood. The dissimilarity arises from the condition of total charge neutrality in the two-electrode case and the relaxation of this condition in the one-blocking-electrode case. In the latter, an applied potential may bring in or withdraw mobile charge through the ohmic electrode, making the system as a whole charged. The mobile charge concentration at the blocking electrode for accumulation ($\hat{\psi}_0 > 0$) is $\hat{n}_0 = \hat{n}_\infty e^{\hat{\psi}_0}$, which may reach very high values. This charge concentration is $\hat{n}_\infty e^{\hat{\psi}_0 - \hat{\psi}_a}$, however, in the two-electrode case. From Eqs. (17) and (16) it can be shown that $\hat{n}_0 = \hat{\psi}_0/(1 - e^{-\hat{\psi}_0})$ and $\hat{n}_{0\max} \simeq \hat{\psi}_a - \ln R\hat{n}_\infty$ in the $R = 0$ and $R > 0$ cases, respectively. Thus, in the two-electrode case, $\hat{n}_0$ cannot appreciably exceed $\hat{\psi}_0$ and $\hat{n}_0$ is therefore limited to much smaller values than in the one-electrode case for the same applied potential. Since the maximum field $\hat{E}_0$ is also a function of $(\hat{\psi}_0 - \hat{\psi}_a)$, it will also be much smaller than that in the one-electrode case.

In the succeeding figures, computer-calculated curves are presented showing how the potential varies with distance between the two electrodes.[19]

Since these curves depend on the three independent parameters $\hat{\psi}_0$, R, and L, only a limited picture of the interaction of these parameters on curve shape can be presented here. A more detailed discussion will be published elsewhere.[22]

Fig. 5 shows how the potential depends on normalized position between the electrodes for several applied potentials, zero recombination, and a length of 10 EDL's. The left electrode will always be taken positive in the following graphs, the mobile charge negative in sign, and $\hat{\psi}_0 > 0$. The

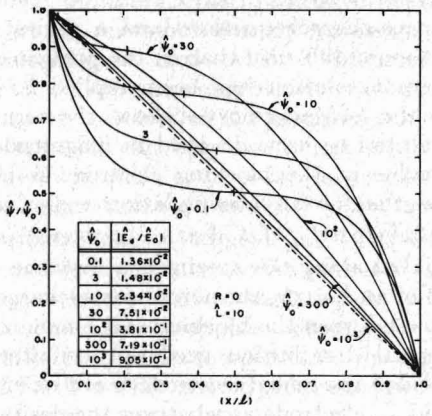

FIG. 5. Dependence of relative potential on relative position between two blocking electrodes for $R = 0$ and various values of $\hat{\psi}_0$.

vertical lines on the curves are placed at the dividing points $(\hat{x}_d/\hat{L}, \hat{\psi}_d/\hat{\psi}_0)$. Note that $x/l = z/L = \hat{x}/\hat{L}$. For very low applied potentials, the potential curve is essentially antisymmetric about $x/l = \hat{x}_d/\hat{L}$, made up of an accumulation portion at the left and an exhaustion portion at the right. Near each electrode the potential depends exponentially on distance from that electrode.

As the applied potential is increased, the potential curves finally approach the linear dependence on distance shown by the diagonal dotted line. In the limit of high potentials, all the mobile charge is concentrated in a region of negligible thickness at the left electrode and the rest of the material is thus exhausted of mobile charge. Under this condition, the electric field is a constant independent of distance and entirely determined by $c_{0\max}$. When the applied potential is less than infinite, the absolute value of the electric field varies monotonically from a common maximum value $|\hat{E}_0|$ at either electrode to a minimum value $|\hat{E}_d| = |\hat{E}(0)| \equiv \theta\sqrt{2c_0}$ at $\hat{x} = \hat{x}_d$. The ratio $|\hat{E}_d/\hat{E}_0)|$ shown in the box in Fig. 5 is a convenient measure of the closeness of approach to constant field and linear potential dependence.

In the next graphs, we shall show potential dependence curves for both a fixed actual length (L and l constant) and for lengths containing a fixed number of EDL's ($\hat{L}$ constant). In this way the two separate effects of increasing recombination ratio can be shown and curves for a wide range of lengths presented.

Fig. 6 shows the situation for $\hat{\psi}_0 = 10$. The figures on the curves are

values of R. Note that $L = \theta\hat{L}$. The curves on the left show what might happen experimentally if R were progressively increased, for example, by decreasing the light intensity on a photoconductor and thereby decreasing its dissociation constant k_1. For fixed length, increasing R causes the potential distribution to become more and more linear because, as shown by the values in the box at the left, the number of EDL's in the length

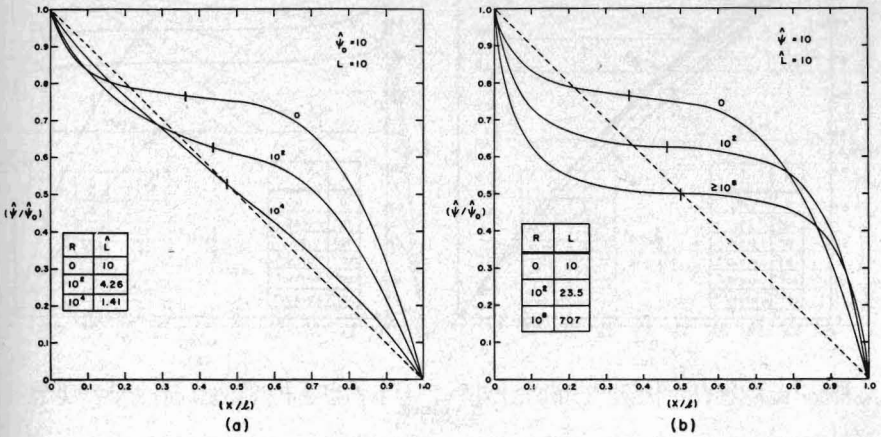

FIG. 6. Potential-distance curves for $\hat{\psi}_0 = 10$ and various R values. The curves in (a) are for a fixed electrode-length independent of R, while those shown in (b) apply for a variable electrode separation of 10 effective Debye lengths.

becomes less and less. The curves on the right show, however, that if the length measured in EDL's is kept constant as R is increased, the effect of increasing R is to decrease $\hat{\psi}_d$ towards $\hat{\psi}_0/2$, to increase $\hat{x}_d$ towards $\hat{L}/2$, and to thereby cause accumulation and exhaustion regions to become more and more antisymmetrical in shape. When full antisymmetry is reached ($e^{\hat{\psi}_d} \ll R\hat{n}_\infty$), as is practically the case for the curve $R \geqslant 10^8$ on the right, the immobile charges have been completely mobilized by a sufficiently large recombination ratio value. Note that the resulting normalized potential distribution is not necessarily identical with that obtained for $R = 0$ and a limitingly small applied potential, (e.g. compare the curve for $\hat{\psi}_0 = 0{\cdot}1$ in Fig. 5).

Fig. 7 shows curves for L and $\hat{L}$ of 10 but for a larger $\hat{\psi}_0$ than Fig. 6. Again for L constant all an increase in R does is cause the curves to approach closer and closer to linearity. It is interesting to note here that even for such large R values that $\hat{L} \ll 1$, the potential curve is not linear until the condition $R\hat{n}_\infty \gg e^{\hat{\psi}_d}$ is satisfied and $\hat{\psi}_d \cong \hat{\psi}_0/2$. As long as this relation is far from being met, the approximate width of the exhaustion region near the cathode is, from Eq. (22), $\theta\hat{x} = z = \sqrt{2\,|\,\hat{\psi}_d\,|}$ when $|\,\hat{\psi}_d\,| \gg 1$. This value of z appreciably exceeds L for Fig. 7 (a), so that the exhaustion region extends over most of the region between electrodes. In this range of R, increases in it can have little effect on the potential distribution because there are no mobile charges to recombine with the fixed charges in the exhaustion region. For constant $\hat{L}$, however, it is seen that the curves become less and less linear as R increases. Since $\hat{\psi}_0$ is large, much larger values of R are required to achieve antisymmetry than in Fig. 6.

Figs. 8 and 9 are for $\hat{\psi}_0$'s of 10 and 100 again but for values of L and $\hat{L}$ of 100 instead of 10. In Fig. 8 the increased value of L requires larger values of R before L becomes unity or less. For those curves without the vertical line denoting the dividing point between accumulation and exhaus-

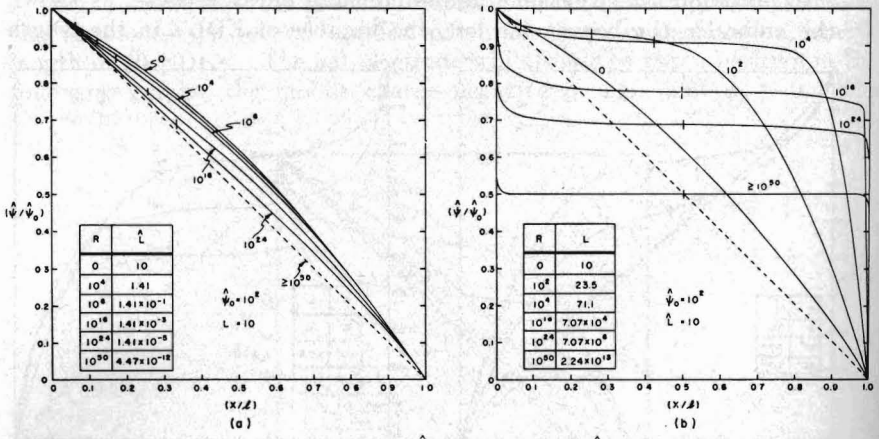

FIG. 7. Potential-distance curves for $\hat{\psi}_0 = 100$, L and $\hat{L}$ equal to 10, and various R values.

tion (or, for sufficiently large R, of accumulation of negative charges on one side, positive charges on the other), the value of c_0 is much less than 10^{-10} and the right and left parts of the curves showing appreciable variation of $\hat{\psi}$ have been calculated separately using $c_0 = 0$. This is an excellent approximation in such cases. Physically, $\hat{L}$ is sufficiently large that exhaustion and accumulation regions are localized near the electrodes and there exists

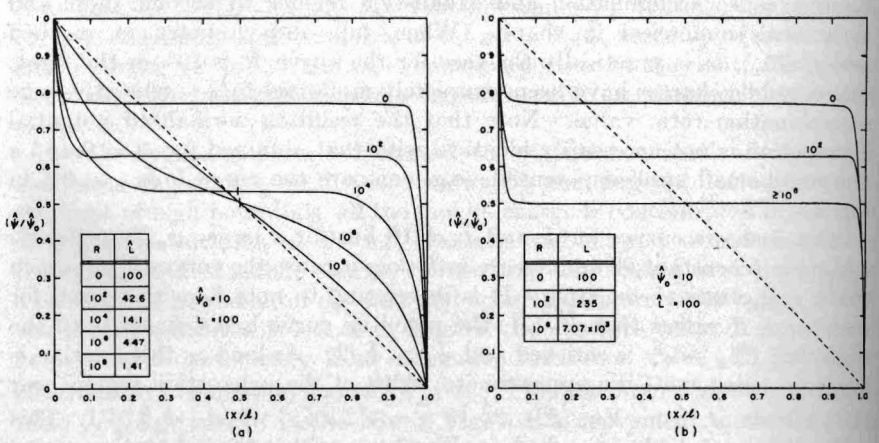

FIG. 8. Potential-distance curves for $\hat{\psi}_0 = 10$, L and $\hat{L}$ equal to 100, and various R values.

an appreciable center region where there is virtually no space-charge. Thus, whenever the potential curves show a substantially flat center region, the one-blocking-electrode, infinite-length solutions may be applied for potential differences of $\hat{\psi}_0 - \hat{\psi}_d$ on the left and $-\hat{\psi}_d$ on the right.

It will be noted from Fig. 9 that if R is not too great almost all of the applied potential drop takes place very near the cathode. In the anti-symmetrical case, the immobile charges are mobilized through recombination and the resulting curves are exactly the same as those obtained from the

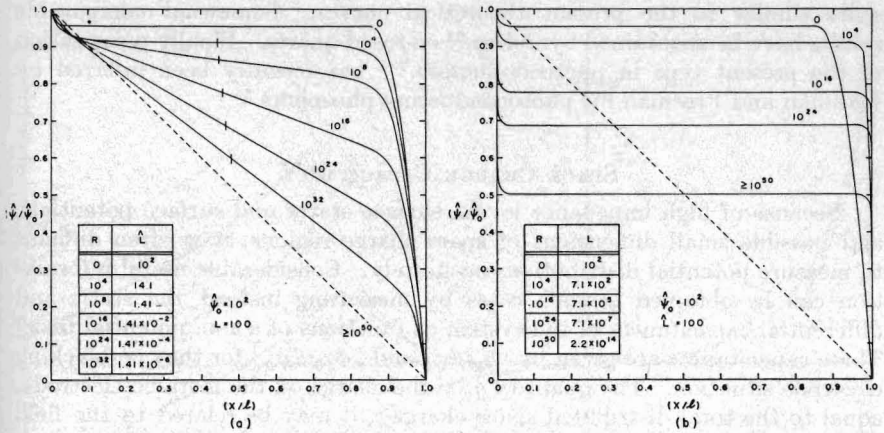

FIG. 9. Potential-distance curves for $\hat{\psi}_0 = 100$, L and $\hat{L}$ equal to 100, and various R values.

Jaffé solution [2, 18] for charges of both signs mobile. It will usually be preferable to use either the computer or approximate solutions to calculate potential distributions in this case because of the inadequate tabulation of the Jacobian elliptic functions required by the Jaffé results. Finally,

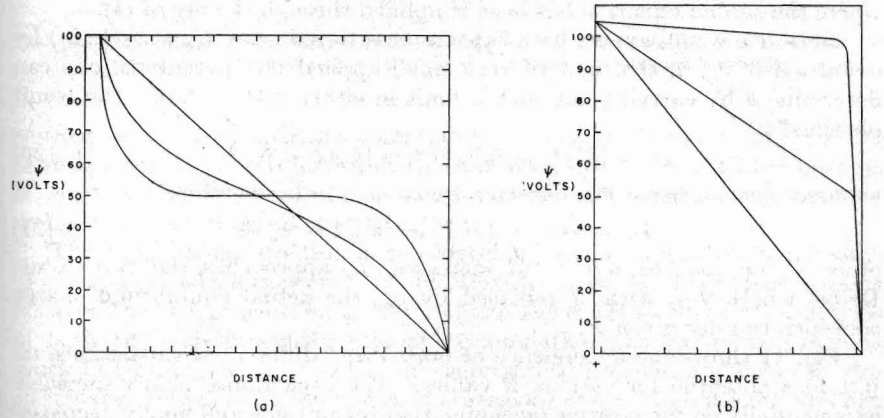

FIG. 10. Experimental potential-distance curves obtained by Joffé[23] for (a) quartz, (b) calcite.

it is worth pointing out that when R is very large the material is essentially an insulator. For a value of N of 10^{20} cm^{-3} and $R = 10^{50}$, the equilibrium charge concentration n_∞ is only 10^{-5} cm^{-3}. Thus, in most cases of interest R will be considerably less than 10^{50}.

Fig. 10 shows some experimental curves of Joffé [23] for heated quartz

(10 (a)) and calcite (10 (b)). Immediately on applying an external potential the linear curves were obtained while the others were observed at subsequent times as polarization built up. Although these curves were drawn from only a few measured points and pertain to an incompletely blocking case since some conduction current was flowing, they show general features quite similar to the present theoretical curves. Somewhat comparable results have been obtained by Cohen [24] on fused quartz. Finally polarization of the present type in photoconductors [7, 8] has recently been inferred by Kallman and Freeman for photoconducting phosphors.[25]

Space Charge Capacitance

Because of high impedance levels, surface states and surface potentials, and possible small dimensions of space-charge regions, it is often difficult to measure potential distributions accurately. Considerable useful information can be obtained in such cases by measuring instead the static and differential capacitances of the system as functions of a D.C. potential bias.[3] These capacitances are given by $| q_0/\psi_0 |$ and $| dq_0/d\psi_0 |$ for the one-blocking electrode situation. The quantity q_0 is the charge on the metallic electrode, equal to the total distributed space charge ; it may be related to the field at the electrode through Gauss's law. One obtains the following expressions for the two capacitances (per unit area) in the case of charge of only one sign mobile in the one-electrode case,

$$C_s = \left(\frac{\epsilon}{4\pi L_e}\right)\left|\frac{\hat{E}(\hat{\psi}_0)}{\hat{\psi}_0}\right| \tag{24}$$

$$C_d = \left(\frac{\epsilon\theta^2}{4\pi L_e}\right)\left|\frac{\hat{n}_0 - \hat{p}_0}{\hat{E}(\hat{\psi}_0)}\right| \tag{25}$$

where the second equation has been simplified through the use of (4).

Since one would expect both capacitances to reduce to $C_0 = (\epsilon/4\pi L_e)$ by definition of L_e in the limit of very small applied D.C. potentials, one can determine θ by carrying out such a limit in either (24) or (25). The result obtained is

$$\theta = [\hat{n}_\infty(1 + R\hat{n}^2_\infty)]^{-\frac{1}{2}} \equiv [\hat{n}_\infty(2 - \hat{n}_\infty)]^{-\frac{1}{2}} \tag{26}$$

as mentioned earlier. The effective Debye length is, therefore,

$$L_e \equiv \theta L_{D_1} = [\epsilon kT/4\pi e^2 n_\infty(2 - \hat{n}_\infty)]^{\frac{1}{2}} \tag{27}$$

Since $\hat{n}_\infty$ approaches zero as R increases, L_e approaches the two-mobile Debye length L_{D2} with N replaced by n_∞, the actual equilibrium charge concentration for given R.

Fig. 11 shows the dependence of normalized differential capacitance on D.C. bias potential for various R values. The capacitance finally increases exponentially on the positive (accumulation-region) side and finally decreases as $| \psi_0 |^{-\frac{1}{2}}$ for large negative potentials (depletion-exhaustion region). The odd behavior for negative $\hat{\psi}_0$ and appreciable R arises from the mobilization of fixed charge by recombination. The height of the peaks are given quite closely by $R^{1/4}/\sqrt{10}$, and thus their measurement should afford a convenient and accurate method of determining R. The static capacitance curves are similar to the differential ones but the peaks occur at somewhat more negative potentials.

In many cases, it may not be possible to form a blocking electrode on a charge-containing material without providing a charge-free insulating region between the material and the electrode. Such a region may be especially necessary for one or both applied polarities when the mobile carriers are electrons or holes. This region will have a potential-independent capacitance

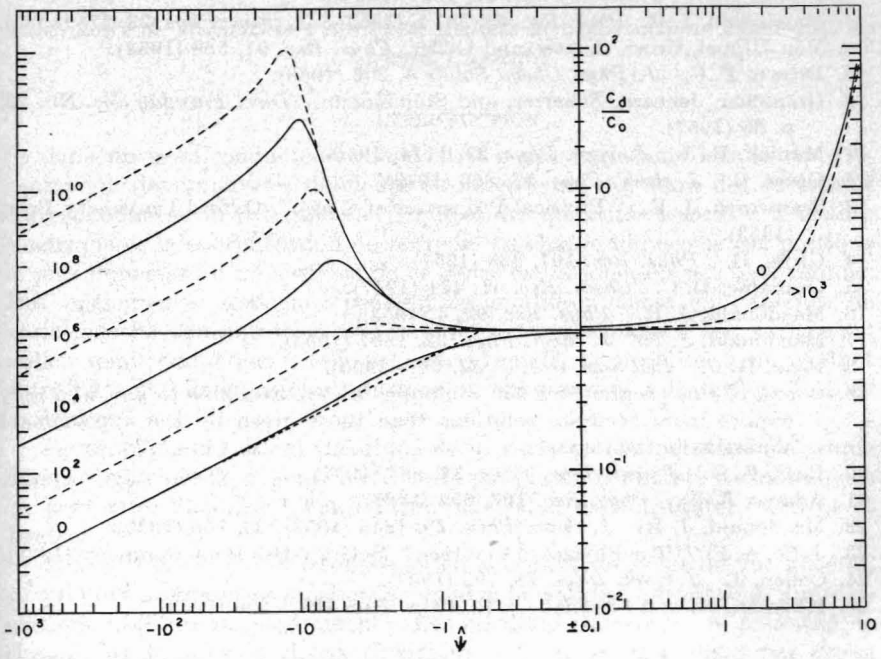

FIG. 11. Normalized differential capacitance of material with a single blocking electrode versus positive and negative applied potential for various R values.

essentially in series with the potential-dependent space-charge capacitance of the material. The behavior of the combined system is of added interest in connection with capacitance measurements on barrier-layer rectifiers and is discussed in detail elsewhere.[22]

The capacitance situation is considerably more complicated in the two-blocking-electrode situation. In addition to possible charge-free regions between the charge-containing material and the electrodes, the capacitances of both the simultaneously present accumulation and exhaustion regions must be considered as well as the geometrical capacitance between the electrodes. These matters are outside the scope of the present work and are discussed in a further paper.[22]

ACKNOWLEDGMENT

The author is most grateful to J. B. Harvill for sustained aid in finding and correcting errors in the several I.B.M. 650 computer programs required for the present work and for invaluable help in programming procedures.

References

1. Macdonald, J. R. *J. chem. Phys.* **23**, 2308 (1955).
2. Jaffé, G. *Ann. Phys., Lpz.* **16**, 217 (1933).
3. Macdonald, J. R. *J. chem. Phys.* **22**, 1317 (1954).
4. Macdonald, J. R. and Brachman, M. K. *J. chem. Phys.* **22**, 1314 (1954).
5. Skinner, S. M. *J. appl. Phys.* **26**, 498 (1955).
6. Friauf, R. J. *J. chem. Phys.* **22**, 1329 (1954).
7. Macdonald, J. R. *Phys. Rev.* **85**, 381 L (1953) ; *J. chem. Phys.* **23**, 275 (1955).
8. Von Hippel, Gross, Jelatis, and Geller, *Phys. Rev.* **91**, 568 (1953).
9. Brown, F. C. *J. Phys. Chem. Solids* **4**, 206 (1958).
10. Gränicher, Jaccard, Scherrer, and Steinemann. *Disc. Faraday Soc.* No. 23, p. 50 (1957).
11. Munick, R. J. *J. appl. Phys.* **27**, 1114 (1956).
12. Gross, B. *J. chem. Phys.* **17**, 866 (1949).
13. Stanworth, J. E. " Physical Properties of Glass." Oxford University Press (1953).
14. Gross, B. *Phys. Rev.* **107**, 368 (1957).
15. Grahame, D. C. *Chem. Rev.* **41**, 441 (1947).
16. Macdonald, J. R. *Phys. Rev.* **92**, 4 (1953).
17. Macdonald, J. R. *J. chem. Phys.* **22**, 1857 (1954).
18. Prim, R. C. *Bell Syst. tech. J.* **32**, 665 (1953).
19. Copies of this program for 650 computer use are available to any who may require more accurate solutions than those given by the approximate equations in the text.
20. Bass, F. G. *J. exp. theor. Phys.* **32**, 863 (1957).
21. Adams, E. N. *Phys. Rev.* **107**, 698 (1957).
22. Macdonald, J. R. *J. chem. Phys.* **29**, 1346 (1958); **30**, 806 (1959).
23. Joffé, A. F. " The Physics of Crystals." McGraw-Hill Book Company (1928).
24. Cohen, J. *J. appl. Phys.* **28**, 795 (1957).
25. Kallman, H. and Freeman, J. R. *Phys. Rev.* **109**, 1506 (1958).